Published May 23, 2005

A mutation in dynein rescues axonal transport defects and extends the life span of ALS mice

Dairin Kieran,[1] Majid Hafezparast,[3] Stephanie Bohnert,[4] James R.T. Dick,[1] Joanne Martin,[5] Giampietro Schiavo,[4] Elizabeth M.C. Fisher,[2] and Linda Greensmith[1]

[1]Sobell Department of Motor Neuroscience and Movement Disorders and [2]Department of Neurodegenerative Disease, Institute of Neurology, London WC1N 3BG, England, UK
[3]Department of Biochemistry, University of Sussex, Brighton BN1 9QG, England, UK
[4]Molecular Neuropathobiology Laboratory, Cancer Research UK, London Research Institute, London WC2A 3PX, England, UK
[5]Neuroscience Centre, ICMS, Queen Mary University of London, The Royal London Hospital, London E1 1BB, England, UK

Amyotrophic lateral sclerosis (ALS) is a fatal neurodegenerative condition characterized by motoneuron degeneration and muscle paralysis. Although the precise pathogenesis of ALS remains unclear, mutations in Cu/Zn superoxide dismutase (SOD1) account for ~20–25% of familial ALS cases, and transgenic mice overexpressing human mutant SOD1 develop an ALS-like phenotype. Evidence suggests that defects in axonal transport play an important role in neurodegeneration. In *Legs at odd angles* (*Loa*) mice, mutations in the motor protein dynein are associated with axonal transport defects and motoneuron degeneration. Here, we show that retrograde axonal transport defects are already present in motoneurons of SOD1^{G93A} mice during embryonic development. Surprisingly, crossing SOD1^{G93A} mice with *Loa*/+ mice delays disease progression and significantly increases life span in *Loa*/SOD1^{G93A} mice. Moreover, there is a complete recovery in axonal transport deficits in motoneurons of these mice, which may be responsible for the amelioration of disease. We propose that impaired axonal transport is a prime cause of neuronal death in neurodegenerative disorders such as ALS.

Introduction

Amyotrophic lateral sclerosis (ALS) is a fatal neurodegenerative condition characterized by progressive motoneuron degeneration (Brown, 1995; Shaw, 1999; Cleveland and Rothstein, 2001; Rowland and Shneider, 2001). Although the precise etiology of the disease remains unclear, mutations in the enzyme Cu/Zn superoxide dismutase (SOD1) are responsible for ~20% of familial ALS cases (Rosen et al., 1993), and transgenic mice overexpressing human mutant SOD1 develop an ALS-like phenotype (Gurney et al., 1994; Wong et al., 1995). The pathological mechanisms that cause selective motoneuron degeneration in ALS remain unclear, but evidence suggests that disruptions in axonal transport may play a significant role (Williamson and Cleveland, 1999; Rao and Nixon, 2003; Jablonka et al., 2004). Indeed, defects in anterograde axonal transport are one of the earliest pathologies observed in SOD1 mice (Williamson and Cleveland, 1999).

Cytoplasmic dynein is a molecular motor involved in retrograde axonal transport along microtubules (Goldstein and Yang, 2000) and plays a central role in motoneuron survival. Mice with a mutation in the dynein heavy chain (*Dnchc1* mutants termed *Legs at odd angles* mice [*Loa*]) show defects in retrograde axonal transport and motoneuron survival (Hafezparast et al., 2003). Inhibition of dynein-mediated axonal transport, by postnatal overexpression of the motor-protein dynamitin, also results in motoneuron degeneration (LaMonte et al., 2002). Furthermore, mutations in dynactin, a motor protein involved in dynein-mediated transport, have been identified in families with slowly progressive forms of ALS (Puls et al., 2003; Munch et al., 2004). Defects in dynein-dependent transport also reduce trafficking of activated Trks, resulting in degeneration of sensory neurons (Heerssen et al., 2004). Thus, impairments of dynein-mediated axonal transport result in neuron degeneration, although some reports suggest that impaired axonal transport may be beneficial (Couillard-Despres et al., 1998; Williamson et al., 1998; Kong and Xu, 1999, 2000).

We studied the consequences of crossing *Loa* mice bearing a mutation in cytoplasmic dynein with SOD1^{G93A} mice. We examined whether interaction between mutant SOD1 and the

Correspondence to Linda Greensmith: l.greensmith@ion.ucl.ac.uk

Abbreviations used in this paper: ALS, amyotrophic lateral sclerosis; EDL, extensor digitorum longus; *Loa*, Legs at odd angles; F.I., fatigue index; PCNA, proliferating cell nuclear antigen; SOD1, superoxide dismutase; TeNT H_C, carboxy-terminal fragment of tetanus neurotoxin; WT, wild-type.

The online version of this article includes supplemental material.

© The Rockefeller University Press $8.00
The Journal of Cell Biology, Vol. 169, No. 4, May 23, 2005 561–567
http://www.jcb.org/cgi/doi/10.1083/jcb.200501085

Supplemental Material can be found at:
http://www.jcb.org/cgi/content/full/jcb.200501085/DC1

THE JOURNAL OF CELL BIOLOGY

Downloaded from www.jcb.org on September 25, 2008

Published May 23, 2005

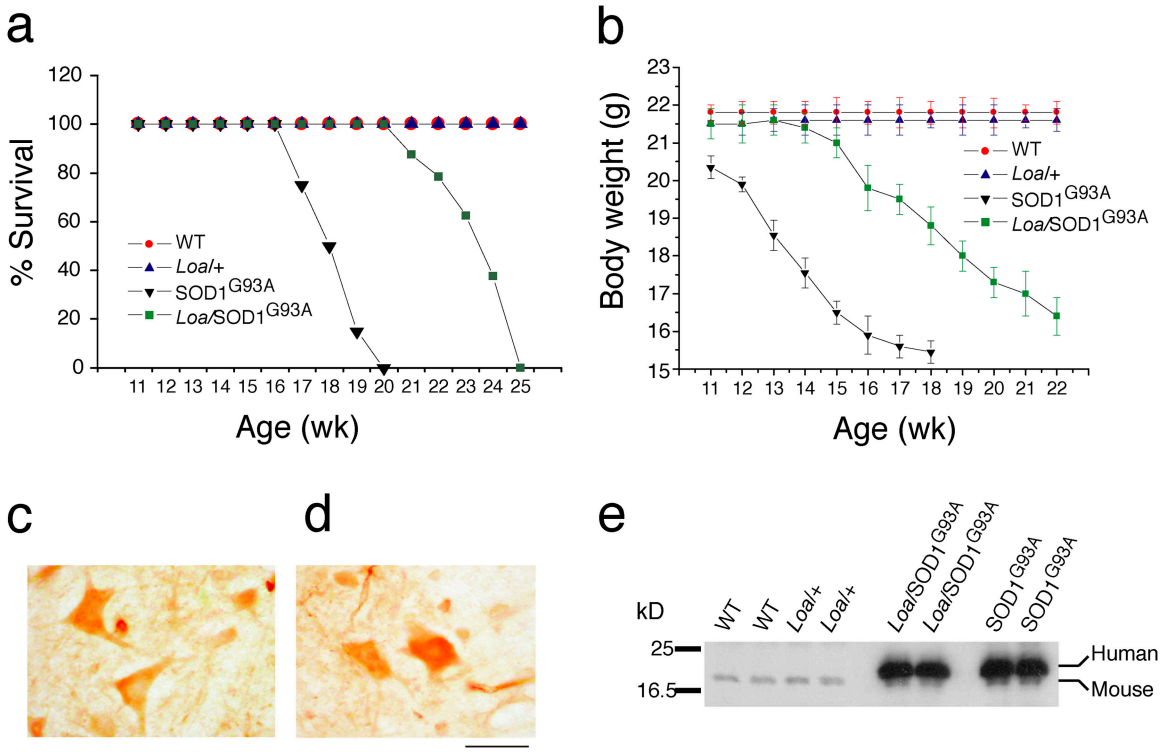

Figure 1. **Life span, weight loss, and expression of human SOD1 transgene.** The graphs show (a) the increase in life span and (b) delayed loss of body weight in the *Loa*/SOD1^{G93A} mice (n = 18–20). Examples of spinal cord sections from SOD1^{G93A} and *Loa*/SOD1^{G93A} mice (c and d, respectively) immunostained for human SOD1 (bar = 70 μm). (e) A representative Western blot of human SOD1 using brain tissue.

dynein mutation would affect disease progression and life span in double-heterozygote (*Loa*/SOD1^{G93A}) mice.

Results and discussion

Loa heterozygote female mice (n = 12) were crossed with SOD1^{G93A} males (n = 10), producing four genetically distinct groups of littermates: wild-type (WT), Loa heterozygotes, SOD1^{G93A} hemizygotes, and Loa/SOD1^{G93A} double heterozygotes. All mice were identified by genotyping for mutations in the *Dnchc1* gene (*Loa* mutation) and the human SOD1 transgene, performed at 21 d and repeated in adults (>120 d).

We examined whether the mutation in cytoplasmic dynein, inherited from Loa mice, altered the life span of SOD1^{G93A} mice (Fig. 1 a). As previously reported, Loa/+ mice had a normal life span (Hafezparast et al., 2003) and SOD1^{G93A} mice a significantly reduced life span of only 125 d (± 2.5 SEM, n = 20), with disease end-stage defined as a loss of the righting reflex and 20% body weight. Surprisingly, *Loa*/SOD1^{G93A} mice lived for 160 d (± 3.1 SEM, n = 18), an increase in life span of 28% ($P \leq 0.001$). Disease onset was also delayed in *Loa*/SOD1^{G93A} mice (see Online supplemental material for description of disease progression and Videos 1 and 2; available at http://www.jcb.org/cgi/content/full/jcb.200501085/DC1) with a significant delay in the loss of body weight (Fig. 1 b).

In view of this delay in disease onset and increased life span of Loa/SOD1^{G93A} mice, we examined the heritability and phenotype of the mutant SOD1 transgene from the *Loa*/SOD1^{G93A} double-heterozygous animals by breeding *Loa*/+ females with *Loa*/SOD1^{G93A} males. SOD1^{G93A} progeny from this cross showed the same phenotype as SOD1^{G93A} mice from the regular F1 (C57BL/6 × SJL) hybrid background, with no difference in life span ($P \leq 0.05$; Achilli et al., 2005).

The expression of the human SOD1 protein was examined to ensure that the breeding protocol had not altered the expression levels of the SOD1 transgene. Spinal cords from each group were processed for immunocytochemistry and quantitative Western blot analysis (Fig. 1, c–e). Human SOD1 was only present in spinal cords of SOD1^{G93A} and *Loa*/SOD1^{G93A} mice, and not WT or *Loa*/+ littermates, as would be predicted by their genotype. Expression levels of human SOD1 in the *Loa*/SOD1^{G93A} mice and their SOD1^{G93A} littermates were quantified by chemifluorescence (ECF) and chemiluminescent (ECL) systems followed by scanning for fluorescence and image analysis, using mouse SOD1 proteins and proliferating cell nuclear antigen (PCNA) as internal standards. We compared the relative fluorescence ratios of mutant SOD1 over mouse SOD1 or PCNA in each genotype with that of the other genotypes. There were no significant differences in these ratios, indicating that the expression levels of the mutant SOD1 protein in each group of mice was the same and was not reduced in *Loa*/SOD1^{G93A} mice.

Disease phenotype and progression in each group of mice was also examined by in vivo physiological analysis of extensor digitorum longus (EDL), an ankle flexor muscle, in 120-d-old mice (Fig. 2). In *Loa*/+ mice at this stage EDL muscles produce a normal force, but in SOD1^{G93A} mice they are significantly weaker ($P \leq 0.05$). Surprisingly, in *Loa*/

Downloaded from www.jcb.org on September 25, 2008

Published May 23, 2005

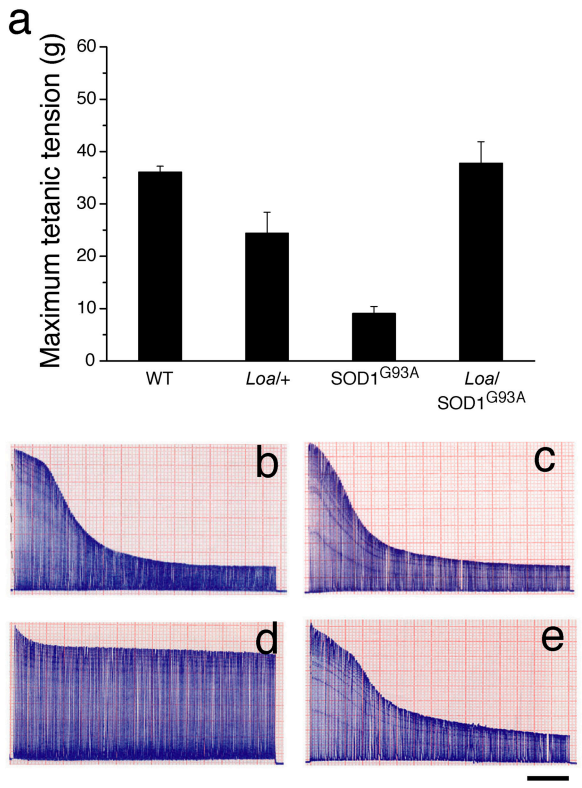

Figure 2. **Muscle force and phenotype.** (a) Maximum force generated by EDL muscles (n = 10–12) in each group at 120 d of age (g = grams). Error bars = SEM. Fatigue traces from EDL muscles of (b) WT, (c) *Loa*/+, (d) SOD1^{G93A}, and (e) *Loa*/SOD1^{G93A} mice at 120 d of age (bar = 30 s).

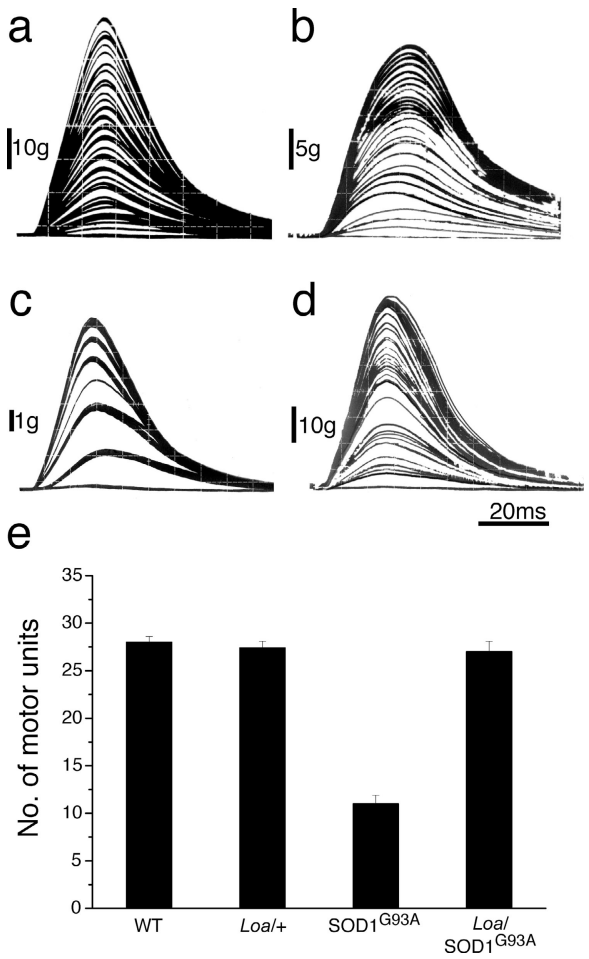

Figure 3. **Motor unit survival.** Examples of motor unit traces from EDL muscles (n = 10) in (a) WT, (b) *Loa*/+, (c) SOD1^{G93A}, and (d) *Loa*/SOD1^{G93A} mice. (e) Mean motor unit survival in each group at 120 d of age. Error bars = SEM.

SOD1^{G93A} mice the muscles are as strong as in WT mice (P = 0.213). Furthermore, changes in the contractile characteristics of EDL that occur during disease progression in SOD1^{G93A} mice (Kieran et al., 2004) do not occur in *Loa*/SOD1^{G93A} mice at this age. EDL is normally a fast-contracting muscle that fatigues rapidly when repeatedly stimulated, producing a characteristic fatigue pattern from which a fatigue index (F.I.) can be calculated. A F.I. approaching 1.0 indicates that a muscle is very fatigable. As can be seen in Fig. 2 and Table I, these characteristics change dramatically in SOD1^{G93A} mice, and by 120 d EDL is a slow, fatigue-resistant muscle. These changes are reflected in alterations in the histochemical properties of the muscle fibers, which show an increase in oxidative capacity, staining darkly for the oxidative enzyme succinate dehydrogenase (Fig. S1, a–d; available at http://www.jcb.org/cgi/content/full/jcb.200501085/DC1). In contrast, in 120-d *Loa*/SOD1^{G93A} mice EDL retains its normal contractile and fatigue characteristics, with no change in muscle fiber phenotype.

Table I. **Contractile and fatigue characteristics of EDL muscles**

	TTP	1/2 RT	F.I.
	ms	*ms*	
WT (n = 10)	25.1 ± 3.0	25.8 ± 2.4	0.85 ± 0.03
Loa/+ (n = 10)	31.2 ± 2.3	32.4 ± 3.9	0.82 ± 0.04
SODG93A (n = 12)	44.5 ± 3.8	86.5 ± 6.0	0.41 ± 0.06
Loa/SODG93A (n = 10)	27.8 ± 1.0	30.0 ± 3.8	0.72 ± 0.04

Table I shows the time taken to reach maximum twitch force (time to peak, TTP), the half-relaxation time (1/2 RT), and the fatigue index (F.I.) of EDL muscles of mice from each cohort of littermates at 120 d of age. Values are ± SEM.

These improvements in muscle function in *Loa*/SOD1^{G93A} mice are reflected in an increase in motor unit survival. Examples of motor unit traces from EDL are shown in Fig. 3, a–d, and mean motor unit survival is summarized in Fig. 3 e. In WT mice, 28 motor units (± 0.6 SEM, n = 6) innervate EDL, which is the same in *Loa*/+ mice (27 ± 0.7 SEM, n = 6). In 120-d SOD1^{G93A} mice only 11 (± 0.9 SEM, n = 6) motor units survive, but in *Loa*/SOD1^{G93A} mice there is a significant increase in motor unit number, and 27 (± 1.1 SEM, n = 6) survive.

There was also a significant increase in motoneuron survival in spinal cords of *Loa*/SOD1^{G93A} mice (Fig. 4). In 120-d SOD1^{G93A} mice only 242 (± 9.6 SEM, n = 8) motoneurons survive in the segment of the sciatic motor pool examined, compared with 608 (± 12.7 SEM, n = 8) in WT mice. In *Loa*/SOD1^{G93A} mice there is a significant increase in motoneuron survival, and 560 (± 15 SEM, n = 8; P ≤ 0.001) survive. There is no motoneuron loss in *Loa*/+ mice at this stage. However, immunostaining of spinal cord sections for glial fibrillary astrocytic protein (GFAP), an astrocyte marker and indicator of the gliosis

Downloaded from www.jcb.org on September 25, 2008

Published May 23, 2005

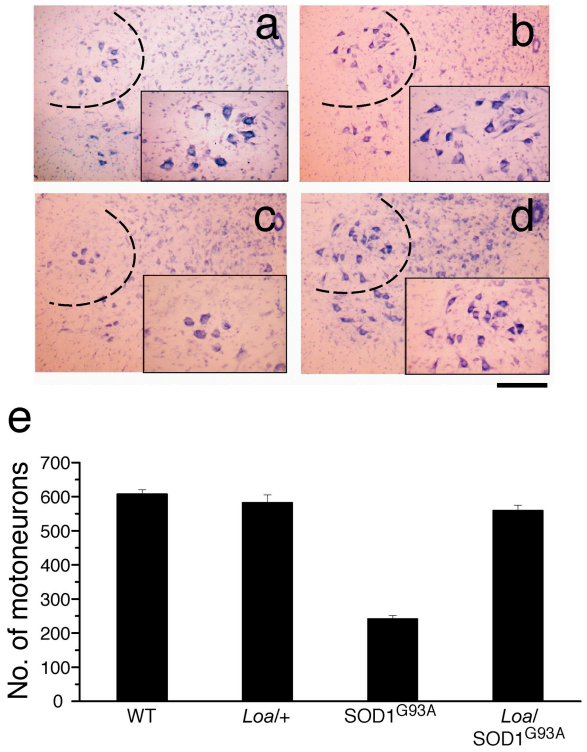

Figure 4. **Motoneuron survival.** Cross sections of spinal cord showing motoneurons in the sciatic motor pools (dotted areas, magnified in insets) from (a) WT, (b) *Loa/+*, (c) $SOD1^{G93A}$, and (d) *Loa*/$SOD1^{G93A}$ littermates at 120 d of age ($n = 8$). Bar: 400 μm (main panels), 200 μm (insets). (e) Mean motoneuron survival at 120 d of age. Error bars = SEM.

that occurs around degenerating motoneurons (Nagata et al., 1998), showed that GFAP was up-regulated not only in spinal cord of $SOD1^{G93A}$ mice, but also *Loa*/$SOD1^{G93A}$ mice, in which no motoneuron death was observed at this time (Fig. S1, e–h).

Because the dynein mutation results in defects in retrograde axonal transport in motoneurons of *Loa/Loa* embryos (Hafezparast et al., 2003), the present results suggest that the onset and progression of disease in $SOD1^{G93A}$ mice may be delayed by further disruption of retrograde axonal transport. To examine whether retrograde axonal transport was altered in motoneurons of *Loa*/$SOD1^{G93A}$ mice, primary motoneuron cultures from spinal cords of E13 littermate embryos of all four genotypes were prepared (Arce et al., 1999) and analyzed using an in vitro retrograde transport assay based on the carboxy-terminal fragment of tetanus neurotoxin (TeNT H_C; Lalli and Schiavo, 2002; Hafezparast et al., 2003; Lalli et al., 2003). This fragment binds specifically to motoneurons and is recruited to a vesicular compartment targeted to the cell body. TeNT H_C carriers, which use both cytoplasmic dynein and myosin Va for their retrograde movement, are shared by both the NGF and the low affinity neurotrophin receptor $p75^{NTR}$. For this in vitro retrograde transport assay, motoneurons were incubated with Alexa 488–labeled TeNT H_C and the transport of the TeNT H_C carriers was monitored in real time (Fig. 5 a; Videos 3–6, available at http://www.jcb.org/cgi/content/full/jcb.200501085/DC1). SOD^{G93A} motoneurons displayed slower and fewer TeNT H_C carriers than WT, *Loa/+*, and *Loa*/$SOD1^{G93A}$ motoneurons (Table S1). $SOD1^{G93A}$-derived TeNT H_C carriers also show a higher frequency of pauses (Fig. 5 a, arrows) and anterograde phases (Fig. 5 a, arrowheads). The corresponding displacement graphs derived from WT, *Loa/+*, $SOD1^{G93A}$, and *Loa*/$SOD1^{G93A}$ motoneurons further confirmed differences in the dynamics of TeNT H_C carriers in $SOD1^{G93A}$ and *Loa*/$SOD1^{G93A}$ (Fig. 5 b; Fig. S2). These differences were quantified by analyzing the speed distribution profiles shown in Fig. 5 c, which were obtained from 144 carriers (1,488 single movements) from three WT embryos, 111 carriers ($n = 1{,}040$) from three Loa/+ embryos, 127 carriers ($n = 1{,}630$) from four $SOD1^{G93A}$ embryos, and 144 carriers ($n = 1{,}163$) from two Loa/$SOD1^{G93A}$ embryos (see Table S1). The vast majority of movements of TeNT H_C carriers are retrograde and are shown conventionally as positive. Surprisingly, even at E13, a relatively early stage of embryonic development, kinetic analysis of this compartment revealed that motoneurons derived from $SOD1^{G93A}$ littermates already displayed an impairment of retrograde transport (Fig. 5, b and c). In particular, $SOD1^{G93A}$ carriers are characterized by an increased frequency of pauses and oscillatory movements (as shown by an increased rate of events in the speed range of −0.2/0.2 μm/s) and by a shift in their speed profile toward lower values (Fig. 5 c; $SOD1^{G93A}$, black line vs. WT, red line). *Loa/+* motoneurons displayed a speed profile very similar to that seen in WT mice (Fig. 5 c, blue line vs. red line; see also Fig. S2), suggesting that two copies of a mutated dynein heavy chain are required to observe the dramatic alteration in retrograde transport previously detected in *Loa/Loa* homozygous mice (Hafezparast et al., 2003). Surprisingly, the deficit in carrier frequency and retrograde transport observed in $SOD1^{G93A}$ motoneurons is completely rescued in *Loa*/$SOD1^{G93A}$ cells in which we observed a decrease in the frequency of pauses and a shift in the speed profile toward higher values. (Fig. 5 c, *Loa*/$SOD1^{G93A}$, green line vs. $SOD1^{G93A}$, black line; see also Fig. S2). This recovery went beyond expectation; the frequency of the carriers was increased and retrograde transport speeds exceeded on average those observed in WT motoneurons.

These results show that a defect in axonal transport is present in motoneurons from $SOD1^{G93A}$ embryos as early as 13 d of gestation. This is one of the earliest reported changes associated with mutant SOD1 expression, and emphasizes the role that disruptions in axonal transport may play in ALS pathogenesis. Surprisingly, this impairment in axonal transport in $SOD1^{G93A}$ motoneurons is completely rescued in motoneurons of *Loa*/$SOD1^{G93A}$ mice. Our results therefore indicate that axonal transport defects play a critical role in motoneuron degeneration in $SOD1^{G93A}$ mice and that rescuing these defects can have a clear beneficial effect both on motor abilities and life span. The unexpected improvement in *Loa*/$SOD1^{G93A}$ mice may occur by rescuing the balance between anterograde and retrograde transport in double-heterozygote motoneurons. Thus, the amelioration of disease in *Loa*/$SOD1^{G93A}$ mice may result from the restoration of axonal homeostasis (i.e., the equilibrium between proximal versus peripheral cargo distribution), or by rescuing an imbalance between positive and negative axonal transport inputs. The modulation of negative retrograde signals may be particularly important in $SOD1^{G93A}$ mice, as

Downloaded from www.jcb.org on September 25, 2008

Published May 23, 2005

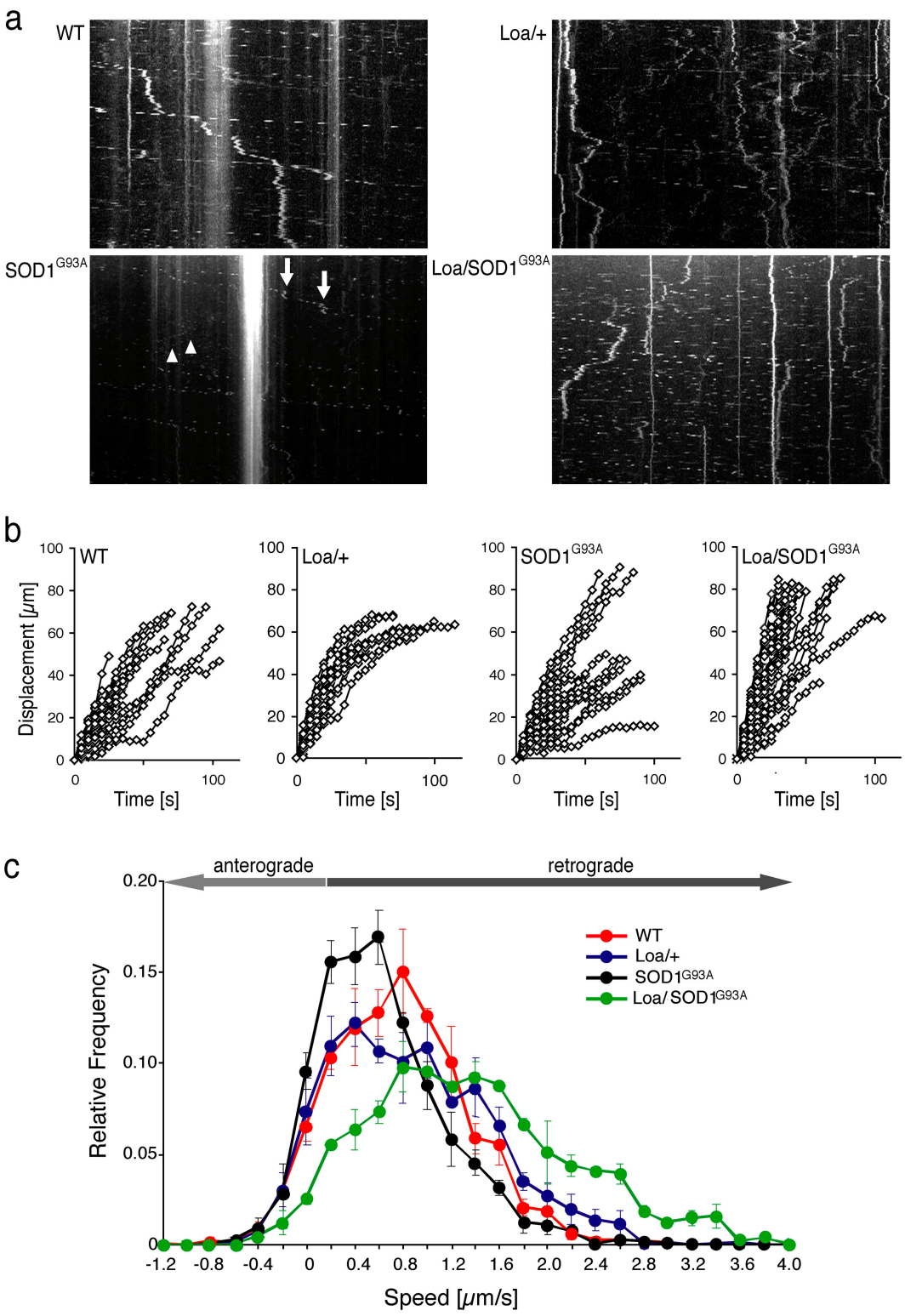

Figure 5. **Kinetic analysis of retrograde axonal transport.** The kymographs show the traces of TeNT H_C–positive compartments in motoneuron axons from WT, *Loa*/+, SOD1^{G93A}, and *Loa*/SOD1^{G93A} primary cultures (a). The width of kymographs corresponds to 65 μm of axon length. The relative abundance of stationary and oscillating TeNT H_C carriers is not related to their genotype. Arrows show paused carriers; arrowheads show anterograde phases. See also Videos 3–6 (available at http://www.jcb.org/cgi/content/full/jcb.200501085/DC1). (b) Displacement of TeNT H_C–positive compartments shown in panel a. The start of tracking for each carrier was set to time = 0. (c) Speed distribution of the TeNT H_C–positive carriers in motoneurons from WT, *Loa*/+, SOD1^{G93A}, and *Loa*/SOD1^{G93A} E13 embryos. Single movements of TeNT H_C–488 carriers, which are described by their progress between two consecutive frames, have been plotted against their frequency. Retrograde transport is conventionally shown as positive, anterograde as negative, and pauses during movement are grouped at 0 μm/s. Error bars = SEM.

Downloaded from www.jcb.org on September 25, 2008

Published May 23, 2005

suggested by the beneficial effects observed after peripheral axotomy (Kong and Xu, 1999) or impairment of $p75^{NTR}$ and neurotrophin-dependent signaling cascades (Reichardt and Mobley, 2004). Alternatively, it is possible that the dynein mutation results in abnormal intracellular transport, which in turn may change the interaction of mutant SOD1 with organelles such as mitochondria, thus delaying cell death. Indeed, it has been suggested that the recruitment of mutant SOD1 to spinal cord mitochondria underlies mutant SOD1-mediated toxicity (Liu et al., 2004). Moreover, mutant SOD1 can bind to mitochondria and form aggregates that recruit the anti-apoptotic protein Bcl-2 (Pasinelli et al., 2004).

In common with many other neurodegenerative diseases, the molecular processes responsible for neuronal death in ALS remain largely unknown. Although the molecular mechanism by which the dynein mutation induces amelioration in *Loa*/$SOD1^{G93A}$ mice is still under investigation, it is clear that the specific impairment of the neuronal function of cytoplasmic dynein rescues the defect observed in $SOD1^{G93A}$ mice and produces a complete recovery of the axonal retrograde transport defect. This in turn may be responsible for the dramatic delay in disease progression and extension in life span observed in *Loa*/$SOD1^{G93A}$ mice.

Materials and methods

The experiments were performed under license from the UK Home Office (Animals Scientific Procedures Act 1986), following local ethical review.

Breeding protocol

Loa/+ heterozygote female mice ($n = 12$) were crossed with $SOD1^{G93A}$ males ($n = 10$) to produce four genetically distinct groups of littermates: WT, *Loa*/+ heterozygotes, $SOD1^{G93A}$ hemizygotes, and *Loa*/$SOD1^{G93A}$ double-heterozygote mice (Achilli et al., 2005). All mice were identified by genotyping for mutations in the *Dnchc1* gene (*Loa* mutation; Hafezparast et al., 2003) and the human SOD1 transgene (Gurney et al., 1994) from tail DNA.

Assessment of muscle force and motor unit number

At 120 d of age, mice were anesthetized (4.0% chloral hydrate solution, 1 ml/100 g body weight, i.p.) and prepared for in vivo assessment of muscle force (Kieran and Greensmith, 2004). Isometric contractions were elicited by stimulating the nerve to EDL using square-wave pulses of a 0.02-ms duration and supramaximal intensity. Contractions were elicited by trains of stimuli at a frequency of 20, 40, and 80 Hz. Twitch, maximum tetanic tension, time to peak, and half-relaxation time values were measured. The number of motor units in both EDL muscles was assessed by applying stimuli of increasing intensity to the motor nerve, resulting in stepwise increments in twitch tension, due to successive recruitment of motor axons.

Fatigue test

EDL muscles were stimulated at 40 Hz for 250 ms every second and the contractions were recorded on a pen recorder (Multitrace 2; Lectromed). The decrease in tension after 3 min of stimulation was measured and the F.I. was calculated as (initial tetanic tension − tetanic tension after stimulation)/initial tetanic tension. A F.I. approaching 1.0 indicates that the muscle is very fatigable.

Muscle histochemistry

EDL muscles were snap frozen and 10-μm serial cross sections were cut and stained for succinate dehydrogenase activity.

Motoneuron survival

After transcardial perfusion with 4% PFA, the lumbar region of the spinal cord was removed and serial 20-μm transverse sections were cut and stained with gallocyanin, a Nissl stain. The number of Nissl-stained motoneurons in the sciatic motor pool of every third section ($n = 60$) between the L2 and L5 levels of the spinal cord were counted. Only large, polygonal neurons with a distinguishable nucleus and nucleolus and a clearly identifiable Nissl structure were included in the counts.

Immunocytochemistry

Sections of spinal cord were immunostained with antibodies to human SOD1 (1:500; Sigma-Aldrich) or glial fibrillary astrocytic protein (1:500; DakoCytomation) using standard protocols.

Microscopy, image acquisition, and manipulation

Spinal cord and muscle sections were examined at RT (22°C) under a light microscope (DMR; Leica) using Leica HC PL Fluotar objectives (10×/0.3, 20×/0.5 and 40×/0.7 magnification/NA). Images were captured using a digital camera (E995; Nikon) and the images downloaded into Adobe Photoshop CS. To optimize image contrast, Levels Adjustment operations were performed, but no other image manipulations were made.

Western blots

Total protein was determined in brain and spinal cord homogenates. NCL-SOD1 (Novocastra Laboratories Ltd.) and anti-PCNA (PC10, Santa Cruz Biotechnology, Inc.) were used to detect mouse/human SOD1 and PCNA proteins, respectively. For SOD1 protein quantification we used the ECF and ECL systems followed by scanning for fluorescence by a Storm-840 scanner (Molecular Dynamics) in three Western blots. Once scanned, the blots were analyzed using FragmeNT analysis software (Molecular Dynamics). Mouse SOD1 and PCNA proteins were used as internal standards to compare the relative amount of mutant SOD1 in each genotype.

Statistical analysis

Statistical significance was assessed between groups using a Kruskal-Wallis test followed by a Mann-Whitney U-test.

Axonal retrograde transport assay

Cysteine-tagged TeNT H_C was labeled with AlexaFluor 488 maleimide (Lalli et al., 2003), and contained 1.8 mol of dye per mol of TeNT H_C. Single embryo cultures enriched in motoneurons were obtained from E13 spinal cords, followed by DNase incubation and centrifugation through a 4% BSA cushion (Arce et al., 1999). This BSA solution was dialyzed for 24 h at 4°C against PBS and 48 h against Leibovitz-15 medium (GIBCO BRL), pH 7.3, using Spectra/Por membranes with a 25-kD cut-off. Cells were resuspended in complete medium, plated onto poly-D,L-ornithine/laminin–coated 35-mm glass-bottom dishes (MatTek) at a density of 60,000 cells/plate, and maintained in culture for 5–7d. Three independent litters were used for the isolation of motoneurons with the four genotypes described. Motoneurons were incubated with 40 nM TeNT H_C-Alexa 488 in complete medium for 30 min at 37°C, washed three times with Dulbecco's minimum essential medium without phenol red, riboflavin, folic acid, and penicillin/streptomycin, and supplemented with 30 mM Hepes-NaOH, pH 7.3. Cells were placed in a humidified chamber maintained at 37°C and were imaged every 5 s with an inverted microscope (Diaphot 300; Nikon) equipped with a Nikon 100×, 1.3 NA Plan Fluor oil-immersion objective. Carrier tracking was performed on time-lapse sequences using Motion Analysis software (Kinetic Imaging). Only moving carriers that could be tracked for at least four time points were considered. The distance covered by a carrier between two consecutive frames (referred to as a single movement) was used to determine its speed. In the final analysis we only included embryos with 15 or more TeNT H_C carriers. Statistical analysis and curve fitting were performed using Microsoft Excel. Kymographs were generated using MetaMorph (version 6.2r4) after rotation of the image stack to align the neuronal process vertically. 200 vertical single-line scans through the center of each process were plotted sequentially for every frame in the time series.

Online supplemental material

The appearance of a number of observable disease features in each group of mice is described in the online supplemental material. Fig. S1 shows the histopathogy of EDL muscles and spinal cord sections of WT, *Loa*/+, $SOD1^{G93A}$, and Loa/$SOD1^{G93A}$ littermates. Fig. S2 shows displacement graphs of TeNT Hc carriers in axons of each cohort of littermates. Table S1 details the kinetic parameters of TeNT Hc compartments in motoneurons of each group of mice. Videos 1 and 2 show examples of 120-d $SOD1^{G93A}$ and *Loa*/$SOD1^{G93A}$ littermates, respectively. Videos 3–6 shows phase images and corresponding movies of TeNT H_C carriers transported in motoneuron axons of mice from each group of mice. Online supplemental material available at http://www.jcb.org/cgi/content/full/jcb.200501085/DC1.

Downloaded from www.jcb.org on September 25, 2008

Published May 23, 2005

We are grateful to The Brain Research Trust, The Motor Neuron Disease Association, The Medical Research Council, and Cancer Research UK for support.

Submitted: 18 January 2005
Accepted: 14 April 2005

References

Achilli, F., S. Boyle, D. Kieran, R. Chia, M. Hafezparest, J.E. Martin, G. Schiavo, L. Greensmith, W. Bickmore, and E.M.C. Fisher. 2005. The SOD1 transgene in the G93A mouse model of amyotrophic lateral sclerosis lies on distal mouse chromosome 12. *Amyotroph. Lateral Scler. Other Motor Neuron Disord.* In press.

Arce, V., A. Garces, B. de Bovis, P. Filippi, C. Henderson, B. Pettmann, and O. deLapeyriere. 1999. Cardiotrophin-1 requires LIFRβ to promote survival of mouse motoneurons purified by a novel technique. *J. Neurosci. Res.* 55:119–126.

Brown, R.H. 1995. Superoxide dismutase in familial amyotrophic lateral sclerosis: models for gain of function. *Curr. Opin. Neurobiol.* 5:841–846.

Cleveland, D.W., and J.D. Rothstein. 2001. From Charcot to Lou Gehrig: deciphering selective motor neuron death in ALS. *Nat. Rev. Neurosci.* 2:806–819.

Couillard-Despres, S., Q. Zhu, P.C. Wong, D.L. Price, D.W. Cleveland, and J.P. Julien. 1998. Protective effect of neurofilament heavy gene overexpression in motor neuron disease induced by mutant superoxide dismutase. *Proc. Natl. Acad. Sci. USA.* 95:9626–9630.

Goldstein, L.S., and Z. Yang. 2000. Microtubule-based transport systems in neurons: the roles of kinesins and dyneins. *Annu. Rev. Neurosci.* 23:39–71.

Gurney, M.E., H. Pu, A.Y. Chiu, M.C. Dal Canto, C.Y. Polchow, D.D. Alexander, J. Caliendo, A. Hentati, Y.W. Kwon, and H.X. Deng. 1994. Motor neuron degeneration in mice that express a human Cu,Zn superoxide dismutase mutation. *Science.* 264:1772–1775.

Hafezparast, M., R. Klocke, C. Ruhrberg, A. Marquardt, A. Ahmad-Annuar, S. Bowen, G. Lalli, A.S. Witherden, H. Hummerich, S. Nicholson, et al. 2003. Mutations in dynein link motor neuron degeneration to defects in retrograde transport. *Science.* 300:808–812.

Heerssen, H.M., M.F. Pazyra, and R.A. Segal. 2004. Dynein motors transport activated Trks to promote survival of target-dependent neurons. *Nat. Neurosci.* 7:596–604.

Jablonka, S., S. Wiese, and M. Sendtner. 2004. Axonal defects in mouse models of motoneuron disease. *J. Neurobiol.* 58:272–286.

Kieran, D., and L. Greensmith. 2004. Inhibition of calpains, by treatment with leupeptin, improves motoneuron survival and muscle function in models of motoneuron degeneration. *Neuroscience.* 125:427–439.

Kieran, D., B. Kalmar, J.R. Dick, J. Riddoch-Contreras, G. Burnstock, and L. Greensmith. 2004. Treatment with arimoclomol, a coinducer of heat shock proteins, delays disease progression in ALS mice. *Nat. Med.* 10: 402–405.

Kong, J., and Z. Xu. 1999. Peripheral axotomy slows motoneuron degeneration in a transgenic mouse line expressing mutant SOD1 G93A. *J. Comp. Neurol.* 412:373–380.

Kong, J., and Z. Xu. 2000. Overexpression of neurofilament subunit NF-L and NF-H extends survival of a mouse model for amyotrophic lateral sclerosis. *Neurosci. Lett.* 281:72–74.

Lalli, G., and G. Schiavo. 2002. Analysis of retrograde transport in motor neurons reveals common endocytic carriers for tetanus toxin and neurotrophin receptor. $p75^{NTR}$. *J. Cell Biol.* 156:233–239.

Lalli, G., S. Gschmeissner, and G. Schiavo. 2003. Myosin Va and microtubule-based motors are required for fast axonal retrograde transport of tetanus toxin in motor neurons. *J. Cell Sci.* 116:4639–4650.

LaMonte, B.H., K.E. Wallace, B.A. Holloway, S.S. Shelly, J. Ascano, M. Tokito, T. Van Winkle, D.S. Howland, and E.L. Holzbaur. 2002. Disruption of dynein/dynactin inhibits axonal transport in motor neurons causing late-onset progressive degeneration. *Neuron.* 34:715–727.

Liu, J., C. Lillo, P.A. Jonsson, C. Vande Velde, C.M. Ward, T.M. Miller, J.R. Subramaniam, J.D. Rothstein, S. Marklund, P.M. Andersen, et al. 2004. Toxicity of familial ALS-linked SOD1 mutants from selective recruitment to spinal mitochondria. *Neuron.* 43:5–17.

Munch, C., R. Sedlmeier, T. Meyer, V. Homberg, A.D. Sperfeld, A. Kurt, J. Prudlo, G. Peraus, C.O. Hanemann, G. Stumm, and A.C. Ludolph. 2004. Point mutations of the p150 subunit of dynactin (DCTN1) gene in ALS. *Neurology.* 63:724–726.

Nagata, Y., K. Fujita, M. Yamauchi, T. Kato, M. Ando, and M. Honda. 1998. Neurochemical changes in the spinal cord in degenerative motor neuron diseases. *Mol. Chem. Neuropathol.* 33:237–247.

Pasinelli, P., M.E. Belford, N. Lennon, B.J. Bacskai, B.T. Hyman, D. Trotti, and R.H. Brown Jr. 2004. Amyotrophic lateral sclerosis-associated SOD1 mutant proteins bind and aggregate with Bcl-2 in spinal cord mitochondria. *Neuron.* 43:19–30.

Puls, I., C. Jonnakuty, B.H. LaMonte, E.L. Holzbaur, M. Tokito, E. Mann, M.K. Floeter, K. Bidus, D. Drayna, S.J. Oh, et al. 2003. Mutant dynactin in motor neuron disease. *Nat. Genet.* 33:455–456.

Rao, M.V., and R.A. Nixon. 2003. Defective neurofilament transport in mouse models of amyotrophic lateral sclerosis: a review. *Neurochem. Res.* 28:1041–1048.

Reichardt, L.F., and W.C. Mobley. 2004. Going the distance, or not, with neurotrophin signals. *Cell.* 118:141–143.

Rosen, D.R., T. Siddique, D. Patterson, D.A. Figlewicz, P. Sapp, A. Hentati, D. Donaldson, J. Goto, J.P. O'Regan, and H.X. Deng. 1993. Mutations in Cu/Z superoxide dismutase gene are associated with familial amyotrophic lateral sclerosis. *Nature.* 362:59–62.

Rowland, L.P., and N.A. Shneider. 2001. Amyotrophic lateral sclerosis. *N. Engl. J. Med.* 344:1688–1700.

Shaw, P.J. 1999. Motor neurone disease. *BMJ.* 318:1118–1121.

Williamson, T.L., and D.W. Cleveland. 1999. Slowing of axonal transport is a very early event in the toxicity of ALS-linked SOD1 mutants to motor neurons. *Nat. Neurosci.* 2:50–56.

Williamson, T.L., L.I. Bruijn, Q. Zhu, K.L. Anderson, S.D. Anderson, J.P. Julien, and D.W. Cleveland. 1998. Absence of neurofilaments reduces the selective vulnerability of motor neurons and slows disease caused by a familial amyotrophic lateral sclerosis-linked superoxide dismutase 1 mutant. *Proc. Natl. Acad. Sci. USA.* 95:9631–9636.

Wong, P.C., C.A. Pardo, D.R. Borchelt, M.K. Lee, N.G. Copeland, N.A. Jenkins, S.S. Sisodia, D.W. Cleveland, and D.L. Price. 1995. An adverse property of a familial ALS-linked SOD1 mutation causes motor neuron disease characterized by vacuolar degeneration of mitochondria. *Neuron.* 14:1105–1116.

Downloaded from www.jcb.org on September 25, 2008